International Journal of Scientific Reports
Jiang Y et al. Int J Sci Rep. 2021 Jul;7(7):327-339
http://www.sci-rep.com
pISSN 2454-2156 | eISSN 2454-2164

DOI: https://dx.doi.org/10.18203/issn.2454-2156.IntJSciRep20212391

Original Research Article

Passage dependent changes in nuclear and cytoskeleton structures of endothelial cells under laminar shear stress or cyclic stretch

Yizhi Jiang, Nathaniel Witt, Julie Y. Ji*

Department of Biomedical Engineering, Indiana University Purdue University Indianapolis, Indianapolis, USA

Received: 01 April 2021
Accepted: 10 May 2021

***Correspondence:**
Julie Y. Ji,
E-mail: jji@iupui.edu

ABSTRACT

Background: The ability of vascular endothelium to sense and respond to the mechanical stimuli generated by blood flow is pivotal in maintaining arterial homeostasis. A steady laminar flow tends to provide athero-protective effect via regulating endothelial functions, vascular tone, and further remodeling process. As arterial aging appeared to be an independent risk factor of cardiovascular diseases, it is critical to understand the effects of cell senescence on endothelial dysfunction under dynamic mechanical stimuli.
Methods: In this study, we investigated the morphological responses of aortic endothelial cells toward laminar flow or cyclic stretch. Automated image recognition methods were applied to analyze image data to avoid bias. Differential patterns of morphological adaptations toward distinct mechanical stimuli were observed, and the shear-induced changes were found to be more associated with cell passages than that of cyclic strain.
Results: Our results demonstrated that the cytoskeleton and nuclear structural adaptations in endothelial cells toward laminar flow were altered over prolonged culture, suggesting that the failure of senescent endothelial cells to adapt to the applied shear stress morphologically could be one of the contributors to endothelial dysfunctions during vascular aging.
Conclusions: Results indicated that cells were able to adjust their cytoskeleton and nuclear alignment and nuclear shapes in response to the applied mechanical stimuli, and that the shear-induced changes were more dependent on PD levels, where cells with higher PDL were more responsive to external forces.

Keywords: Nucleus, Cytoskeleton, Shear stress, Cyclic stretch, Endothelial cells

INTRODUCTION

Cardiovascular diseases (CVD) have been the leading cause of death in developed countries, contributed to 1 in every 4 death in the United States.[1] Atherosclerosis is the major cause of arterial diseases and was recognized as a chronic inflammatory response to vascular injuries initiated on dysfunctional endothelium.[2] Aging was known to be an independent risk factor in promoting atherosclerosis, however, the mechanism of how vascular aging contributes to CVD is not fully understood yet.

Aging is accompanied with cellular or replicative senescence. Notably, in vascular tissues, the extensive endothelial cell senescence has been found to be present in aged arteries or atherosclerotic plaques, which was concomitant with the alternations in EC structures and functions, such as expanded cell size, polygonal cytoskeleton, increased cell permeability, increased secretion of extracellular proteins and dysregulated expression of vasodilators and adhesive molecules.[3,4] Increased arterial stiffness, cellular sensitivity to pro-inflammatory signals, and vascular cell senescence due to aging effects have all been found to play causative roles in lesion development.[5,6] Atherosclerotic plaques preferentially develop at arterial sites of geometric transitions, such as bifurcations and curvatures.[7,8] These regions are characterized by altered shear pattern and

cyclic strains and increased arterial stiffness.[9-11] Endothelial functions, such as proliferation and apoptosis and production of regulatory molecules are all influenced by the local mechanical environment.[12]

In vivo studies have also suggested a correlation between endothelial morphologies and the local mechanical environment. EC orientation was found to coincide with its local flow directions.[12-14] Endothelial nuclear orientation also appeared less ordered at aorta regions with non-uniform flow.[15] It was proposed that these remodelling processes due to mechanical stimuli provided a feedback to maintain endothelial homeostasis, while unstable disturbance can interfere with the balance and make the local region atheroprone.[16] Cells adapted with structural change in response to the exerted forces that trigger the corresponding mechanosensitive pathways, by interacting with cytoskeleton-associated molecules. Disturbance in nuclear mechanics due to mutations in lamins proteins also led to substantial vascular impairment.[17] The subsequent *in vitro* research revealed that cultured ECs were also responsive to various mechanical stimuli with morphological changes. With cyclic stretch, ECs realigned their cytoskeleton toward the direction with minimized substrate deformation through a mechanism dependent on actin filaments.[18] Most cells reoriented perpendicular to the applied biaxial or uniaxial stretch direction within few hours, and they formed a 'tent-like' structure in response to biaxial stretch, probably through the mechanism involving Ca^{2+} stretch-activated channels.[19] These reorientations were reported to be more affected by stretching magnitude than the rate, and the observations of peripheral vacuoles and pseudopods under high magnitude stretch indicated the role of stretch in EC proliferation and permeability at athero-prone sites.[20-22]

On another hand, EC morphological responses to shear stress were more versatile and dependent on the applied flow pattern considering the complexity of arterial flow patterns. Under prolonged laminar or non-reversing shear flow at high magnitude (above 12 dynes/cm^2), both actin and microtubules filaments tended to be aligned with the flow direction over time, and an intact microtubules network was required for cell shape change.[23] However, ECs subjected to reversing or oscillatory flow, or laminar flow at low amplitude (under 5 dynes/cm^2) mostly remained their polygonal shape.[24,25] These findings demonstrate that ECs were able to discriminate flow patterns through mechanisms differed from that of stretch. And in reality, multiple forces can interact and affect EC morphological changes simultaneously *in vivo*.[26] Aged human umbilical vein endothelial cells (HUVEC) showed declined cell proliferation and viability under bisphenol (an endocrine disruptor) over prolonged culture, and distinctive changes in α-tubulin and nuclear morphology were observed.[27] Increased cell senescence in aged endothelium induced changes in gene expression and impairment in cellular structure and function, which further modified cell phenotypes and accelerated endothelial dysfunction and vascular inflammation.[28]

While it is important to evaluate cellular structural changes under mechanical stimuli to better understand the changes in cell and nuclear mechanics and their associated pathways, these responses must also be evaluated with respect to vascular and endothelium aging. In this study, we addressed the effects of EC proliferative potential on their morphological responses toward physiological cyclic stretch or laminar shear forces. Our results suggest that the shear-induced morphological changes in endothelial cells were more sensitive to cell passage than the modifications directed by stretch force. Overall, shear stress and cyclic stretch have different effects on cell and nuclear remodelling in a passage dependent manner. In addition, we developed image analysis and quantitative tools that can be used for future studies on endothelial functions and nuclear mechanics.

METHODS

Cell culture

Bovine aortic endothelial cells (BAEC, Lonza Company) with limited lifespan were grown in Dulbecco's Modification of Eagle's Medium (DMEM, Corning) containing 10% heat-inactivated fetal bovine serum (JR Scientific), 1% of L-glutamine and 2% penicillin-streptomycin (Cellgro). Cells were maintained in a humidified incubator (37°C, 5% CO_2).

Population doubling level

Population doubling level (PDL) was utilized in our study to estimate the total number of divisions that cells in the population have undergone since their primary isolation *in vitro*. PDL was calculated as log (final cell population/initial cell population)/log 2. We chose to call cell population that has PDL up to 13 after the first passage as 'low', and 'middle' as to have PDL estimated at 45, and 'high' refers to cells with PDL estimated at 60.

Mechanical experiments

To generate laminar flow on the cell monolayer, a parallel plate flow chamber was used as previously described.[29] A custom-made stretch device was designed alternatively to exert uniaxial cyclic stretch on cells. Cells were initially seeded on a silicone membrane pre-coated with fibronectin at 8 μg/ml to assist cell attachment, and the membranes were then transferred to the stretch device and immersed in the culture media during the experiment. The applied shear stress was measured as 2 or 15 dyne/cm^2, and cyclic stretch was applied at 1 Hz with 10% of magnitude. The duration of both mechanical experiments was 6 hours.

Immunostaining

After treatment, cells were fixed in 4% (w/v) paraformaldehyde (PFA) solution for 20 minutes and permeabilized in 0.5% Triton X-100 solution for 15 minutes. Unspecific binding sites were blocked by

incubating cell samples in 1% BSA for an hour. F-actin was stained by Alexa 660 Phalloidin (1:375 dilution in 1% BSA) for an hour, and Hoechst 33342 solution (1:1000 dilution in PBS) for 15 minutes. Fluorescent images were acquired by Leica DMI 6000B fluorescent microscope.

Proliferation assay

Cell proliferation was accessed by using Click-iT EdU Alexia Fluor 594 Imaging Kit (C10339, invitrogen). On day 1, cells were plated on either glass slides or fibronectin-coated silicone membranes, and after 24 hours, cells were exposed to shear stress at low (2 dynes/cm^2) or arterial magnitude (15 dynes/cm^2), or uniform cyclic stretch at 1 Hz, 10% strain for 4 hours. After that, EdU (5-ethynyl-2´-deoxyuridine) was added to the growth medium at 10 µM with incubation time of 2 to 2.5 hours, after which cell were fixed and permeabilized in 3.7% PFA solution and 0.2% Triton X-100, respectively. Cells were incubated in Click-it reaction cocktail for another 30 minutes according to the manufacturer instruction.

To visualize nuclei, cells were further stained by Hoechst 33342 solution for 15 minutes before proceeding to imaging. 15-20 fields of view were randomly chosen for analysis, where each field of view contains about 1000 number of cells, and a custom MATLAB program was developed to recognize and count the number nuclei and proliferating cells.

Finally, proliferation ratio was calculated as the fraction of cells stained positive by Alexa Fluor 594 over total number of cell nuclei stained by Hoechst solution.

Image analysis

Custom MATLAB programs were created to aid in quantifying nuclear morphologies and actin alignment. To identify nuclei, images were converted into greyscale and smoothed with a Gaussian filter before being transformed into black and white binary images.

Any recognized objects within a certain distance of the border or below a size threshold were also removed to avoid partial cells or non-cell objects.

Analysis of the cells began with finding the cell properties: area, perimeter, centroid, major/minor axis length, and orientation, by using MATLAB's region props function.

Circularity was calculated as:

$$\frac{4\pi * area}{perimeter^2}$$

Elongation was calculated by:

$$\frac{\pi * Feret'diameter}{perimeter}$$

Any elongation value greater than 1 indicates that it is the ovoid shape but not increased protrusions that led to the circularity change.[30] Aspect ratio was presented by:

$$\frac{Major\ axis}{Minor\ axis}$$

To confirm cell's elongation. Nuclei below circularity of 0.80 or out of the area range between 40.9 cm^2 to 292 cm^2 were excluded from the data set to avoid overlapping cells and cells undergoing mitosis. Nuclear orientation was represented by the acute angle between Feret's perimeter of nuclei and the horizontal baseline (the direction at which the force was applied). The images were placed such that horizontal direction was parallel to the direction of shear stress or cyclic stretch. As a result, the angle of 0º indicates orientation along the shearing or cyclic stretch direction, and the angle of 90º indicates realignment perpendicular to the direction of applied force. Orientation angles ranged from 0 to 180º in relation to the horizontal axis. To facilitate statistical comparisons as well as presentation of orientations by mean values, the degree of orientation angle was projected from the range of 0 to 180º to the range of 0 to 90º. In other words, angles in the second quadrants are projected into the first quadrants to obtain a mean angle of orientation relative to direction of applied force. For a randomly distributed orientation, the mean angle would be 45º.

The analysis method was adapted from Liu et al to quantify actin filament orientations.[31] Images were filtered and modified in a manner similar to that of nuclei code, with an addition of an edge identification component in order to separate lines from other objects in the image. The selected areas of each image were cropped into a 700-pixel square section, and these new images were then split into 100 equal sub-images. In each sub-image, Hough transform was performed to detect actin filaments, and orientation values were averaged from the orientation of the detected lines and contributed to the overall 100 averages of one section.

Statistical analysis

Data points were presented as mean±SEM. To quantitatively show significant changes, unpaired t-test was performed in two-group comparison, and one-way ANOVA followed by Turkey multiple comparison procedure was performed between groups.

A comparison with p value less than 0.05 was regarded as significant.

RESULTS

PDL had an effect on actin realignment toward shear force, but not cyclic strain

The effect of passage on nuclear and cytoskeleton alignment under mechanical stress were assessed based on

fluorescence image analysis. To obtain the orientation information of the cytoskeleton, cells were fixed and stained for actin filaments using phalloidin which binds to F-actin. Nuclei were stained with Hoechst stain. Figure 1 shows representative images for static control and cells that were sheared (Figure 1A) or stretched (Figure 1B) for 6 hours. Low and high PDL cells under static state or after mechanical loadings are included as demonstration of images that were used for quantitative analysis.

Using custom written MATLAB image analysis codes, we quantified direction of orientation based on actin filaments relative to the direction of shear or stretch. The polarizations of stress fibers at each local area were determined after averaging out the detected orientations from the sub-images. The mean orientation angles of actin filaments for static, sheared and stretched cells for low and high PDL cells were presented in radar plots in Figure 2.

For low PDL cells, shear stress did not alter cytoskeleton orientation at 6 hours (Figure 2A). For high PDL cells, 6 hours of shear stress induced a significant decrease in orientation angle down to 41.2º (Figure 2B). Six-hour shear exposure on endothelial cells did not cause significant actin reorientation (0.5-degree decrease in average) when cells were at low PDL. In other words, actin orientation distributions between control and sheared groups at early PDL were indistinguishable (Figure 2A). However, for high PDL cells, the mean value was shifted toward the shear direction by 6.9 degrees in the same case, and the change was statistically significant (Figure 2B). In addition, shear stress at low level (2 dynes/cm^2), which is typical of areas prone to developing atherosclerosis, did not change actin alignment for middle PDL cells and shifted 2.7 degrees away from the shear direction (Figures 2E and 2F). Interestingly, the ability of 6 hours stretch at 1 Hz with 10% magnitude, in inducing actin polarization was independent of PDL level, with more than 9-degree changes in both cases (Figures 2C and 2D). These reorientations were oblique to the direction of uniaxial stretch force, possibly in a way to minimize the substrate deformation that strain can cause.[18]

The effects of mechanical forces on nuclear orientation mostly coincided with actin realignment

Considering the connections between cytoplasmic and nuclear structure by LINC (linker of the nucleoskeleton and cytoskeleton) complex, it is also worthwhile to examine if the nuclei were reoriented under mechanical forces, and how the potential changes differed from actin realignment or depended on PDL levels.[32] To help quantify nuclear orientation, cells labeled by actin dye were co-stained by Hoechst solution, and fluorescent images were analyzed for nuclear orientation by recognizing the direction of the Feret's diameter through another custom MATLAB program (Figure 3). Using similar analysis as actin filament, orientation angle for static control was measured as 45 degrees, shown as blue lines in each radar plot of Figure 3. Under shear stress, the nuclei were reoriented toward the direction of force by 9 degrees on average for cells at high PDL (Figure 3B), similar to actin; but the trend was not observed in low PDL cells (Figure 3A), with only 2-degree decrease in mean values. However, under cyclic strain, low PDL cells showed 9.6-degree deviation toward the oblique direction (Figure 3C), while high PDL cells had a higher deviation with 13.6 degrees (Figure 3D). Again, shear stress at low level (2 dynes/cm^2), did not alter nuclear alignment significantly for low and middle PDL cells (Figure 3E and 3F).

Combined with results from actin filaments analysis, we could conclude that physiological shear stress and stretch force can have distinct impacts on cytoskeletal and nuclear structure. As expected, shear stress and cyclic stretch had the opposite effect in terms of orientation direction for both actin and nucleus. The effect of shear stress was more dependent on PDL level than cyclic stretch, with greater alignment at higher PDL only. For cells under cyclic stretch, the effect of PDL is more directly felt. These observations may be related to declined proliferative potential with increasing PDL (Figure 6).

Cyclic strain dramatically modified nuclear morphologies regardless of PDL, compared with shear case

To describe nuclear morphologies more specifically, we conducted the measurements of nuclear area, circularity, elongation and aspect ratio, and we also included the middle PDL group into the analysis for better characterization. The nuclear area was reduced upon the exposure to shear stress when cells were at low PDL, i.e.; with higher proliferative potential. However, this reduction became attenuated in middle PDL cells, and the trend was finally reversed in cells with high PDL, even if the nuclei kept expanding over serial subculture (Figure 4A). Interestingly, the low PDL group did not experience area reduction when stretch force was applied, but as PDL went up the area was shown to decrease (Figure 5A). The smaller nuclear area fluctuations in cells seeded on fibronectin-coated softer substrate over passages (Figure 5A) than that on uncoated glass slides may also suggest the effects of ECM molecules or substrate stiffness on cell morphologies. Except for discrete effects on nuclear area, these two forces also gave rise to different changes in other shape factors that were related to cell spreading events. Cells at all PDL levels under cyclic strain showed less circular and more elongated nuclei, which were characterized by decreased circularity and increased aspect ratio (Figure 5B and 5D).[33] Elongation parameter confirmed the correlations between these two factors (Figure 5C). However, cells experienced shear stress for the same duration did not exert significant changes in nuclear roundness or polarization, especially at lower PDL stages (Figure 4B, 4C and 4D), which coincided with the orientation data presented in Figure 2A and 3A. In high PDL group, cells exhibited a significant drop in nuclear circularity at rest state (Figure 4B), but its elevation occurred after shear stress was applied without apparent

change in elongation parameters (Figure 4C and 4D), suggesting that the nuclear protrusions due to prolonged passages can be rescued by applying the shear force. Taken all the results together, we concluded that the exposure of cyclic stretch at physiological levels (10% of magnitude at 1 Hz) can consistently realign cytoskeleton and modify nuclear morphologies for cells at all PDL levels, while applying shear stress at 15 dynes/cm^2 for the same duration of time led to fewer changes in actin orientation and nuclear shape, especially in low PDL group.

Cell proliferation decreases with PDL level, regardless of mechanical stress

Finally, to relate cell's PDL level with proliferative ability, we conducted proliferation assay on low and middle PDL BAEC to confirm decreasing proliferation potential with increasing PDL.

Briefly, cells were exposed to shear stress at low (2 dynes/cm^2) or normal arterial magnitude (15 dynes/cm^2), or cyclic stretch (10% of magnitude at 1 Hz) for 4 hours, and were incubated with EdU (5-ethynyl-2´-deoxyuridine) for another 2 hours before fixation. Overall cells with higher PDL showed reduced proliferation under all conditions. With shear stress, proliferation ratio in lower PDL cells appeared to be more sensitive to shear stress than middle PDL. In low PDL cells, shear stress at either level significantly reduced endothelial proliferation compared to static. At either PDL, shear along reduced proliferation ratio, and the reduction of proliferation is directly related to magnitude of shear (Figure 6 A-C).

For stretched cells, middle PDL cells showed reduced proliferation ratio, compared to low PDL cells. However, adding stretch alone did not reduce proliferation ration compared to static cells at either PDL (Figure 6 D-F). These findings suggest that increasing PDL led to decreased proliferation in endothelial cells; although shear stress further suppressed proliferation in a magnitude dependent matter, while cyclic stretch along did not reduce proliferation.

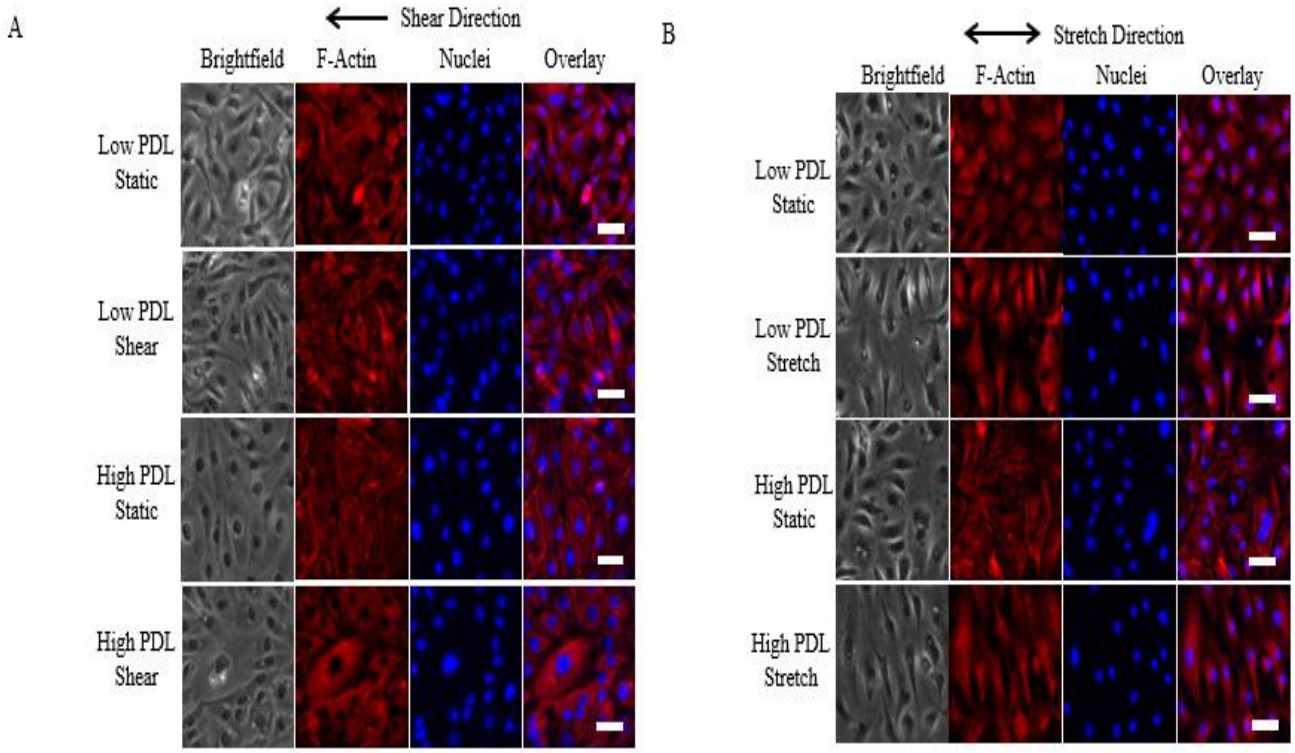

Figure 1: Representative images of low and high PDL cells, labelled for F-actin, and nuclei, with or without the application of laminar shear or cyclic strain (A) static control cells and cells exposed to 6 hours shear stress, from left to right, were shown: in brightfield, stained for F-actin with Alexa 660 phalloidin, stained for nuclei with Hoechst, and overlay of both stains; (B) static control cells and cells exposed to 6-hour cyclic stretch, sideways, were shown: in brightfield, stained for F-actin with Alexa 660 phalloidin, stained for nuclei with Hoechst, and overlay of both stains. Scale bar- 20 µm.

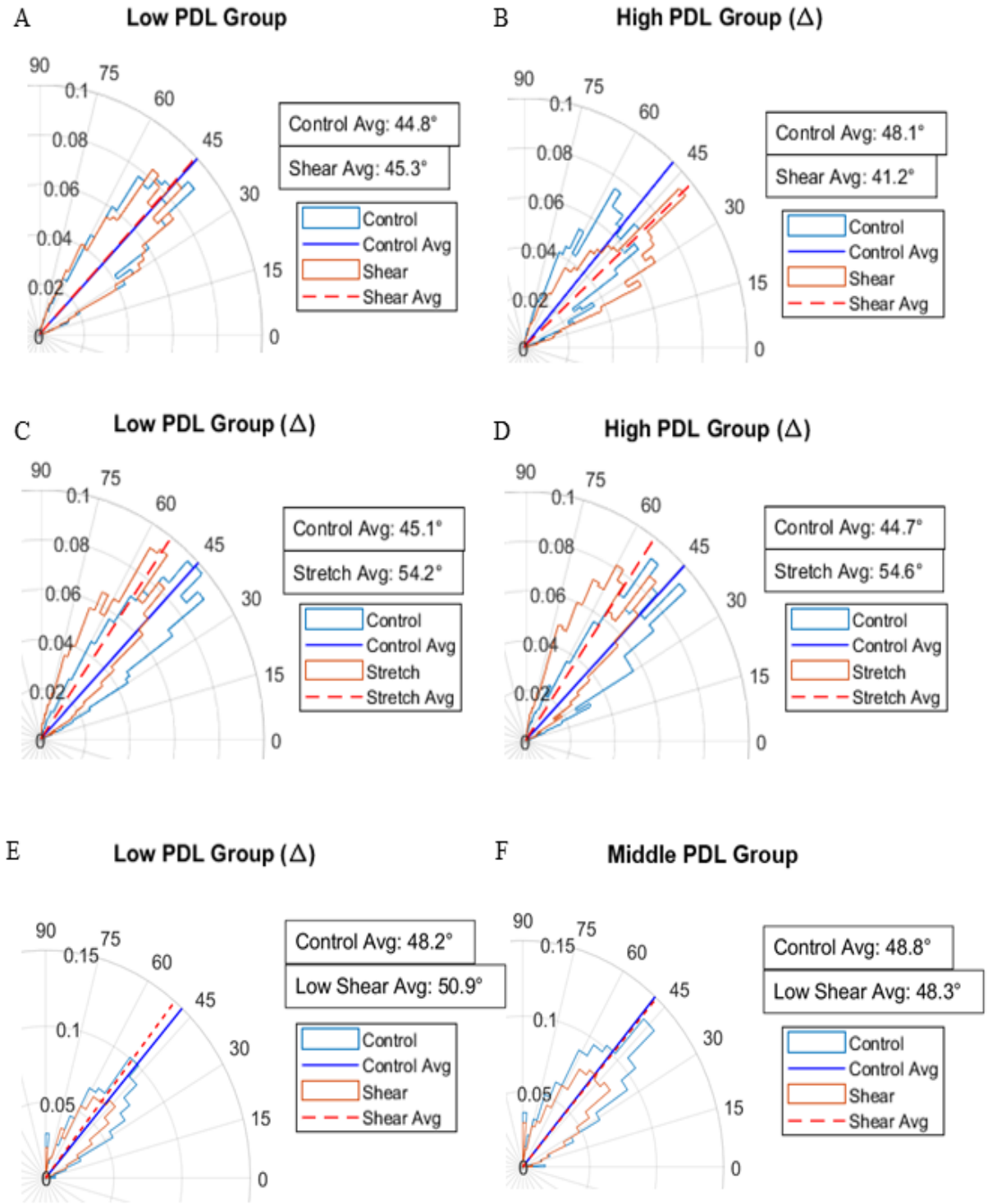

Figure 2: Actin alignments before and after cells were exposed to mechanical forces. Histogram of the angle distribution for cells (A and C) at low; or (B and D) at high PDL was shown in the radial direction including the averages (light blue line for static and yellow dotted line for sheared or stretched cells). Only high PDL group showed realignment parallel to the shear direction (Δ $p<0.001$ compared with the control group); (C and D) changes in the angular distribution of actin orientations in cells at low or high PDL after exposed to cyclic stretch (10% at 1 Hz) were both significant; (E and F). In addition, actin alignment was also quantified for cells at low and middle PDL after exposure to low level shear stress at 2 dynes/cm^2. Orientation angle for static control was measured as 45±3 degrees.

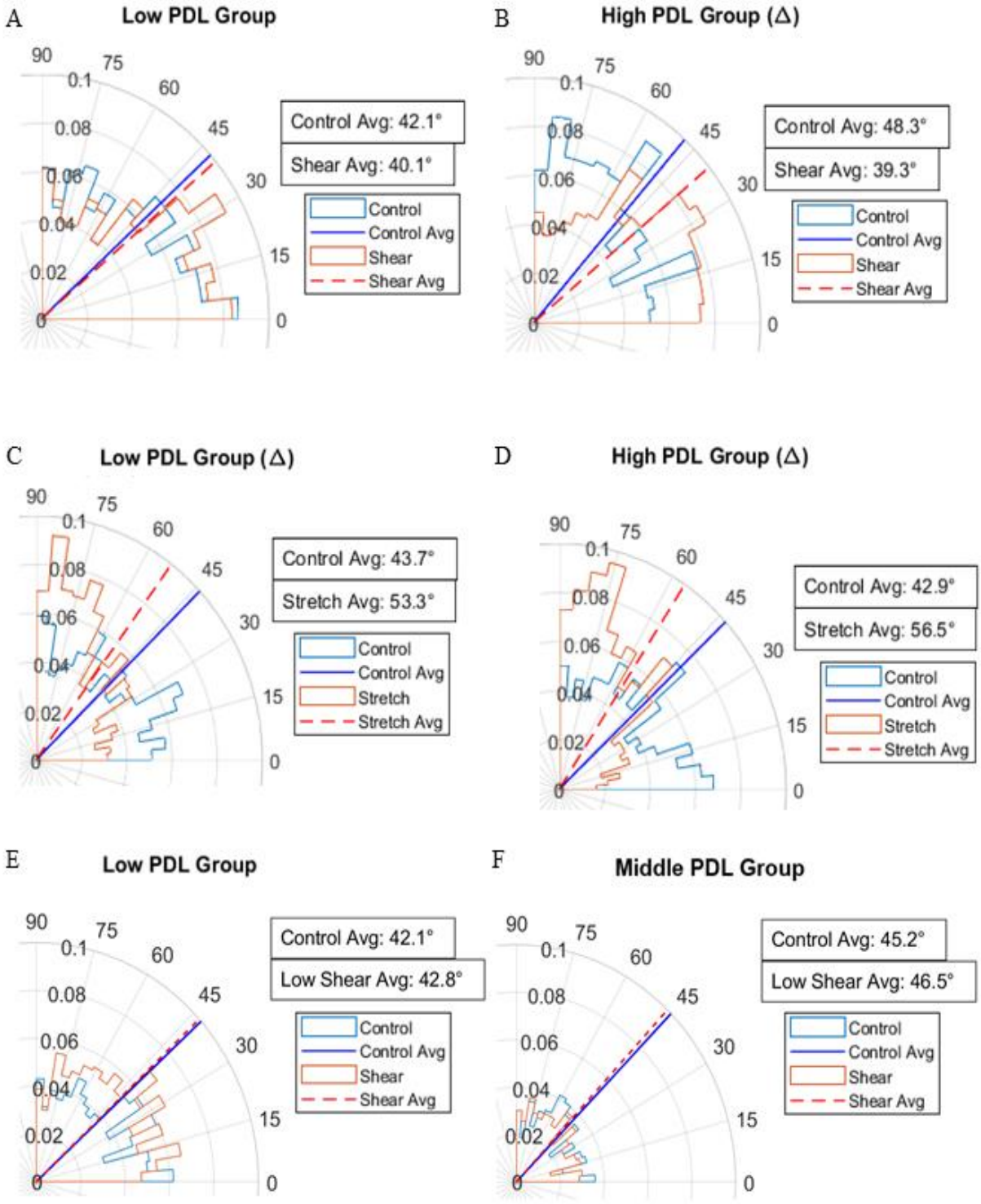

Figure 3: Nuclear orientations before and after cells were exposed to mechanical forces. Similar to the trend observed in for actin, (A) nuclear orientation in low PDL group was not observed after exposed to shear stress; (B) while the average of the nuclear orientations in cells at high PDL was skewed toward the shear direction after the experiment; (C and D) the nuclei in cells at low or high PDL were both observed to be realigned to the direction oblique to cyclic stretch (10% at 1 Hz). (Δ $p<0.001$ compared with the corresponding control group); (E and F) nuclear orientation was also quantified for cells at low and middle PDL after exposure to low level shear stress at 2 dynes/cm^2.

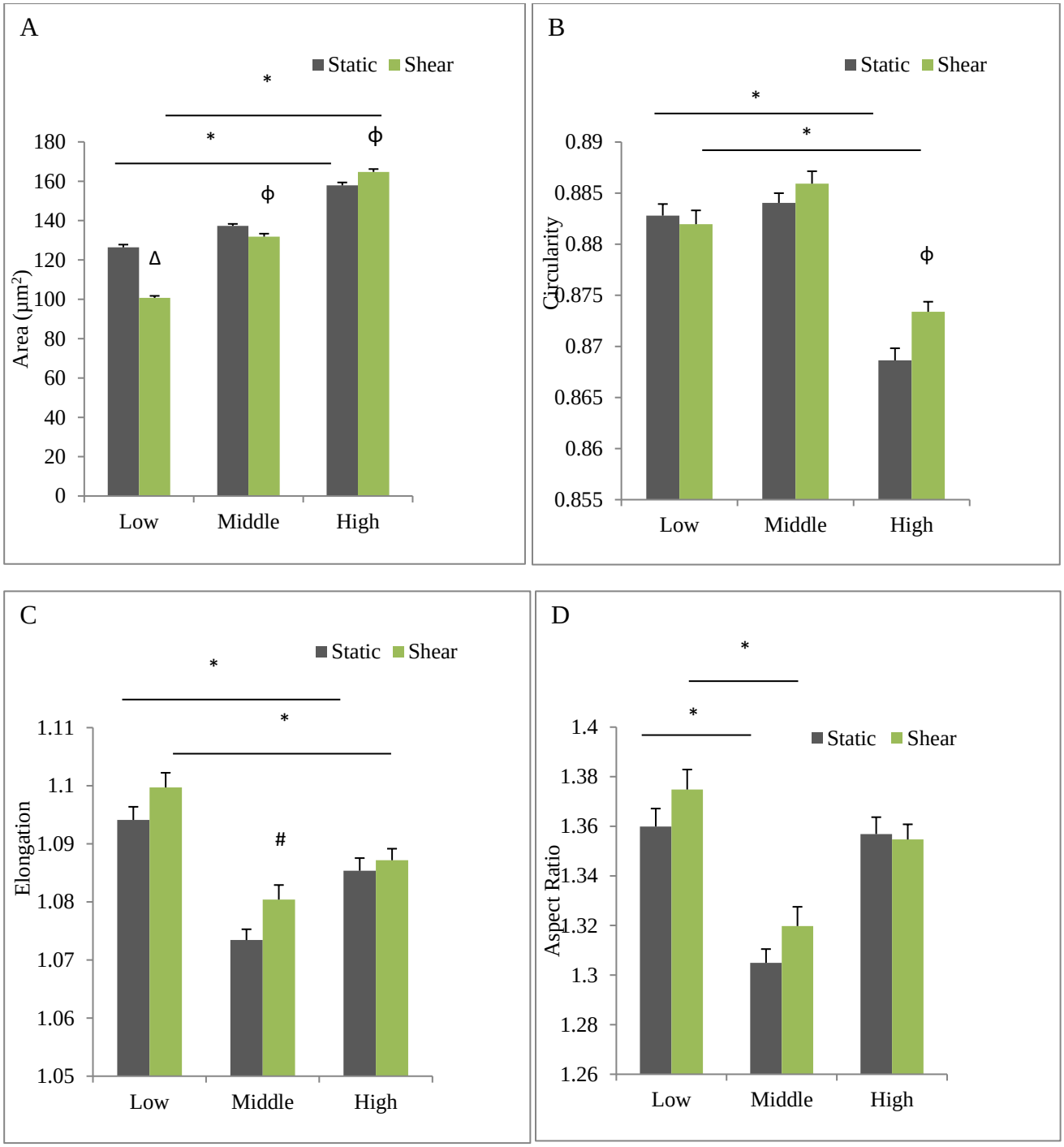

Figure 4: Characteristics of nuclear morphology at different PDL levels before and after exposure to shear stress. (A) Nuclear area (μm2) of cells with varied PDL before and after shear. Cells at lower PDL showed reduced nuclear area after exposed to shear stress (Δp<0.001, φ p<0.01 compared to static controls), while cells at high PDL had area elevated after shear force was applied. High PDL cells also showed increased nuclear area compared with low PDL cells (*p<0.05 compared to cell groups at low PDL); (B) nuclear circularity before and after shear. Although nuclear circularity was largely compromised in high PDL groups (*p<0.05 compared to cell groups at low PDL), the parameter was elevated after exposed to shear (φ p< 0.01 compared to static control); (C) elongation of nuclei with varied PDL before and after shear. Only the nuclei in middle PDL group were elongated after shear (#p<0.05 compared with static group). The elongation was decreased in high PDL groups (*p<0.05 compared to cell groups at low PDL); and (D) aspect ratio of nuclei before and after shear. No significance was observed in any group after shear. However, the ratio was significantly decreased in middle PDL groups (*p<0.05 compared to cell groups at low PDL).

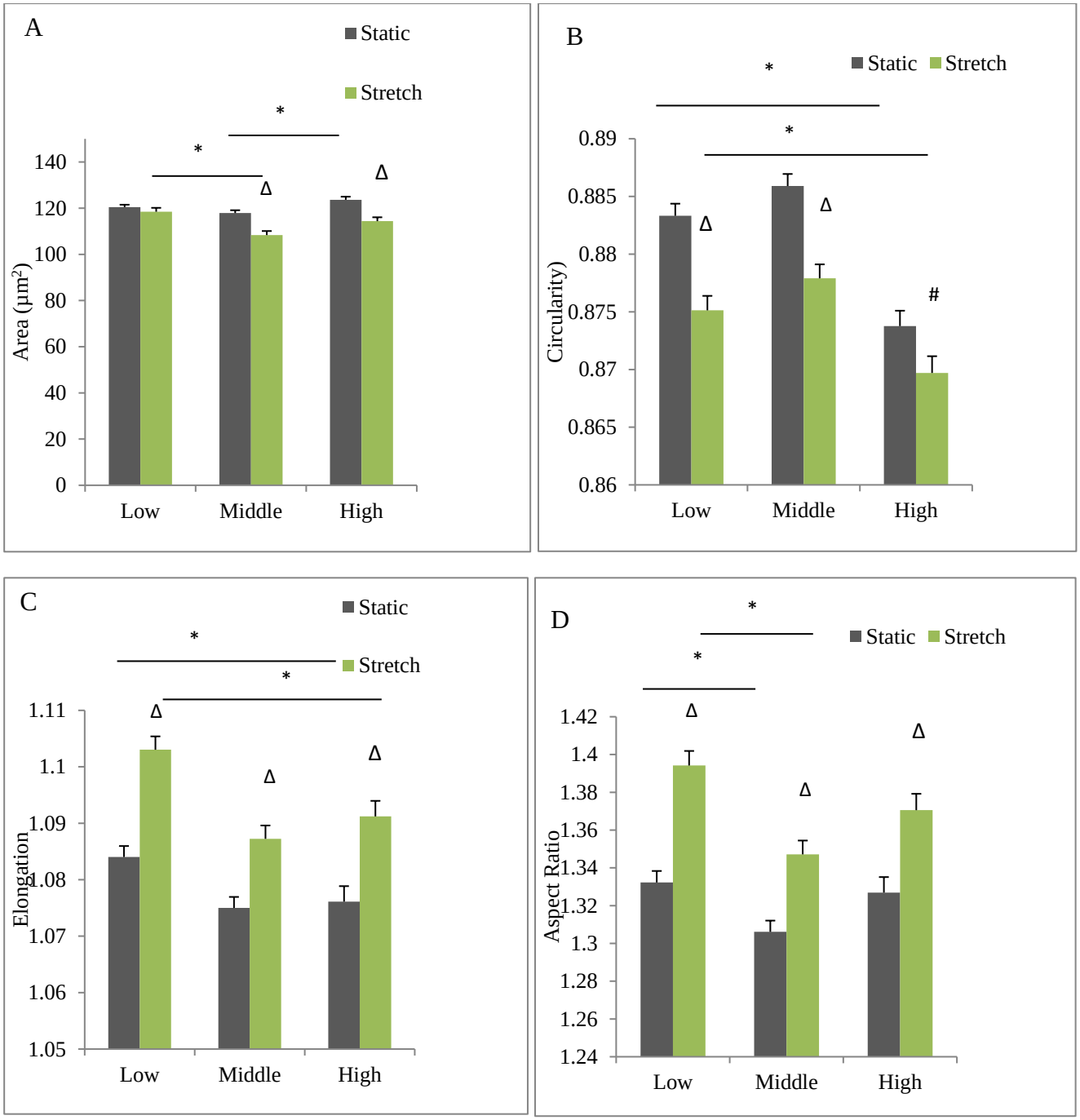

Figure 5: Characteristics of nuclear morphology at different PDL levels before and after exposure to cyclic strain. (A) nuclear area (μm²) of cells with varied PDL before and after shear. Cells at higher PDL showed reduced nuclear area after exposed to stretch force (Δp<0.001 compared to static controls). Area changes between groups at different PDL levels were not conclusive (*p<0.05 for low and middle PDL group after stretch, and middle and high PDL group in static states); (B) nuclear circularity before and after stretch. All groups showed decreased circularity after exposed to stretch force (Δp<0.001 and #p<0.001 compared to static groups), and high PDL cells also showed decreased nuclear area compared with low PDL cells (*p< 0.05 compared to cell groups at low PDL); (C) elongation of nuclei with varied PDL before and after shear. Similar as that of circularity, all groups showed elongated nuclei after exposed to stretch force (Δp<0.001 compared to their corresponding static groups), and high PDL cells were less elongated compared with low PDL cells (*p<0.05 compared to cell groups at low PDL); and (D) aspect ratio of nuclei with varied PDL before and after stretch force. All groups showed increased ratio after exposed to stretch force (Δp<0.001 compared to their corresponding static groups), and low PDL group had lower aspect ratio than groups with higher PDL (*p<0.05 compared to groups at middle PDL).

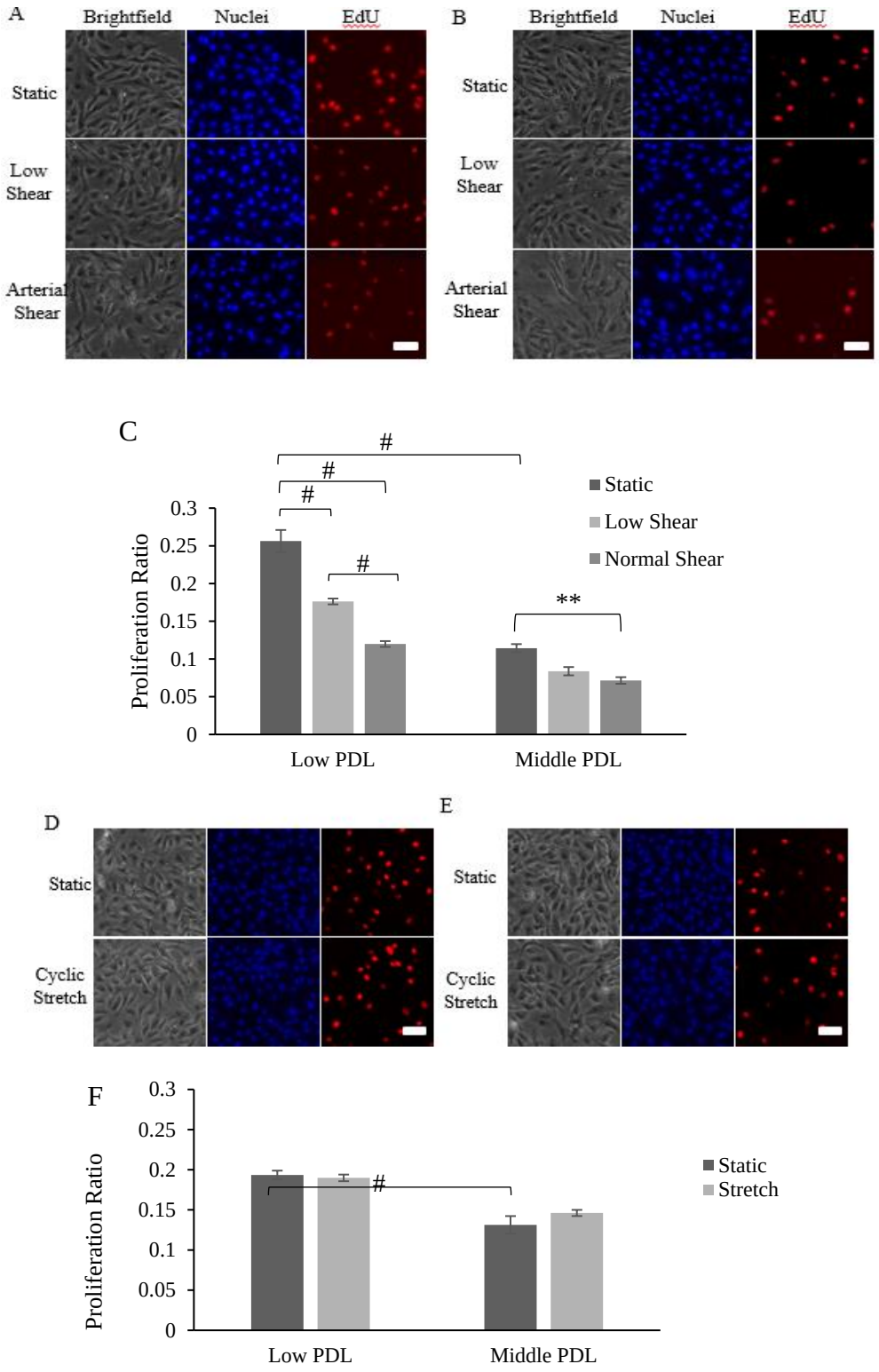

Figure 6: Proliferation ratio of Low and High PDL cells exposed to shear stress at low (2 dynes/cm^2) "Low Shear" or normal arterial magnitude (15 dynes/cm2) "Normal Shear", or "Cyclic Stretch" (10% of magnitude at 1 Hz) for 4 hours. Static control and cells exposed to shear stress, were shown: in brightfield, channels stained for nuclei with Hoechst and with EdU Alexia Fluor 594 for low PDL (A) and middle PDL (B). Based on these images, quantified results of proliferation ratio were calculated for all groups (C). Static control and cells exposed to cyclic stretch, were shown: in brightfield, channels stained for nuclei with Hoechst, and with EdU Alexia Fluor 594 for low PDL (D), and middle PDL (E). Based on these images, quantified results of Proliferation Ratio were calculated for all groups (F). Error bars indicate SEM. One-way ANOVA was performed, and ** P < 0.01, # P < 0.001, between the indicated groups. Scale bar is 50 µm.

DISCUSSION

Our previous study has indicated that EC morphology was sensitive to both fluid shear stress and cell passage, however, the relative small data pool due to manually selections compromised its application.[34] Therefore, we developed customized programs in this study to encompass more data into analysis and to improve the representativeness of the data set. Here, we mainly investigated whether cell senescence had an impact on EC morphological responses towards physiological-related laminar shear stress or cyclic strain, by means of the serial subculture of bovine aorta endothelial cells. The results suggested that, under the same force duration, the morphological modifications in stress fiber and nuclei by 10% cyclic strain at 1 Hz were more consistent over cell passage than that of laminar shear stress at 12 dynes/cm^2, and that the late-passage ECs were more sensitive to laminar shear than the early-passage cells in terms of their morphological responses. Incidentally, low shear stress at 2 dynes/cm^2 had no distinguishable effect on cell or nuclei re-orientation.

We primarily investigated how stress fiber and nuclei were reorganized under the applied mechanical stresses, and if these remodelling events were dependent on PDL. We showed that cell's proliferative ability decreased with PDL level, independent of mechanical stress (Figure 6). Figure 2 and 3 provided information of the reorientations of actin filaments and nucleus under shear stress or stretch force, and we concluded that the realignments brought by shear force were associated with cell passage, while the responses towards cyclic strain were comparatively independent upon PDL.

It is interesting that cells at early PDL subjected to shear stress did not show significant realignment as in other studies, and there might be multiple contributors. The cells that had morphological modifications by shear stress reported in the previous studies were subjected to flow for 24 hours or more, which allows for long-term adaptive changes.[23,25,35] Alternatively, our image analysis omitted the nuclei below the circularity value of 0.80 for the purpose of eliminating non-cell objects or overlapping nuclei, which also filtered out small number of true nuclei with massive elongation under shear. Another important finding of shear-induced changes lies in the trend of cell realignment (Figure 2B and 3B) and nuclear shape modifications under shear stress as PDL got high (Figure 4B). The increase in circularity may come from the beneficial effect of laminar shear on rescuing nuclear protrusions as cells underwent extensive proliferation *in vitro* (Figure 4C), and this result combined with the reorientations in stress fiber and nuclei toward shear indicate that the associated functional changes may also be uniquely induced in high PDL ECs by shear stress.[36]

Comparatively, cell shape changes under uniaxial cyclic strain were consistent over *in vitro* proliferation, and the nuclei of cells at all PDL were elongated and realigned oblique to the stretch direction (Figure 3 and 5), along with the similar reorientation tendency of actin filaments (Figure 2C and 2D) suggest the profound effect of cyclic stretch on modifying cellular structures even when cells were undergoing senescence. The nuclei of control groups showed uniform distribution in orientation angle within all degrees (Figure 3C and 3D), however, after the exposure to 6-hour stretching, nuclei with low degree values, i.e. the nuclei horizontal to the stretch direction dropped significantly regardless of cell PDL, and the distribution was skewed toward the side with larger degrees, with the mean angles changed by 9.6 and 13.6 degrees for low and high PDL groups, respectively.

The data set of actin alignment, on another hand, followed a normal distribution when cells were at rest state, and that was due to the applied analysis method that complied with the Central Limit Theorem, where the orientation value for a certain area was gained through averaging out the orientation angles of sub-images.[37] The mean angles were elevated by 9.1 and 9.9 degrees after stretching experiment in low and high PDL groups, respectively (Figure 2C and 2D). By comparing these actin and nuclear orientation information for cells at the same PD level, we noticed that the degree difference increased from 5.5% to 37.4% as PDL got higher. This poses an indicative change in nucleo-cytoskeletal coupling over aging process, considering the interplay between actin and nuclear dynamics.[38-40]

Except for the cell shape factors discussed above, the nuclear size was also examined for different PDL groups with or without mechanical stress, since it is indicative of DNA content and compactness. The increase of nuclear area over senescence observed in Figure 4A (with 24.6% increase in high PDL cells compared with low PDL group at static state) has been reported in previous studies, which may be correlated with the expansion of cell size over serial culture.[41] However, the cells seeded on less stiff silicone membranes rather than glass slides did not show similar tendency (Figure 5A), even if the visual observation has suggested remarkable cell enlargement through passages, where the ECs populations were dominated by giant polygonal cells instead of spindle-like cells over serial culture. The underlying mechanism could be related to the ECM molecule applied to assist cell attachment, or the change in substrate stiffness.[42] The observed effect of restraining nuclear expansion against cell enlargement over aging demonstrated cells' ability to sense their surroundings and transmit the signal into nucleus in an aging-resist manner. Interestingly, the nuclear size was also associated with the applied stretch or shear in a PDL-dependent manner, and the two dissimilar effects in Figure 4A and 5A also indicated distinct mechanisms of the nuclear area changes under different stresses, where aging process was also involved.

CONCLUSION

Overall, we examined how cell morphology was modified under physiological-related cyclic strain or laminar flow,

and if these changes were associated with cell age. Results indicated that cells were able to adjust their cytoskeleton and nuclear alignment and nuclear shapes in response to the applied mechanical stimuli, and that the shear-induced changes were more dependent on PD levels, where cells with higher PDL were more responsive to external forces. Our studies dissected the roles of replicative senescence and external forces in reshaping cells, and provided evidence that stress-induced changes were not always consistent over prolonged passages, which addressed the necessity of investigating the contribution of the responses from senescence ECs in athero-susceptible sites.

ACKNOWLEDGEMENTS

The authors would like to acknowledge and thank the Department of Biomedical Engineering at IUPUI for their continued support.

Funding: No funding sources
Conflict of interest: None declared
Ethical approval: Not required

REFERENCES

1. Virani SS, Alonso A, Benjamin EJ, Bittencourt MS, Callaway CW, Carson AP, et al. Heart Disease and Stroke Statistics-2020 Update: A Report From the American Heart Association. Circulation. 2020;141(9):139-596.
2. Gimbrone MA, Garcia CG. Endothelial Cell Dysfunction and the Pathobiology of Atherosclerosis. Circ Res. 2016;118(4):620-36.
3. Vasile E, Tomita Y, Brown LF, Kocher O, Dvorak HF. Differential expression of thymosin beta-10 by early passage and senescent vascular endothelium is modulated by VPF/VEGF: evidence for senescent endothelial cells in vivo at sites of atherosclerosis. FASEB J. 2001;15(2):458-66.
4. Kumazaki T, Kobayashi M, Mitsui Y. Enhanced expression of fibronectin during in vivo cellular aging of human vascular endothelial cells and skin fibroblasts. Exp Cell Res. 1993;205(2):396-402.
5. Chung HY, Lee EK, Choi YJ, Kim JM, Kim DH, Zou Y, Kim CH, et al. Molecular inflammation as an underlying mechanism of the aging process and age-related diseases. J Dent Res. 2011;90(7):830-40.
6. Minamino T, Komuro I. Vascular cell senescence: contribution to atherosclerosis. Circ Res. 2007;100(1):15-26.
7. Brown AJ, Teng Z, Evans PC, Gillard JH, Samady H, Bennett MR. Role of biomechanical forces in the natural history of coronary atherosclerosis. Nat Rev Cardiol. 2016;13(4):210-20.
8. Vanderlaan PA, Reardon CA, Getz GS. Site specificity of atherosclerosis: site-selective responses to atherosclerotic modulators. Arterioscler Thromb Vasc Biol. 2004;24(1):12-22.
9. Liang Y, Zhu H, Friedman MH. The correspondence between coronary arterial wall strain and histology in a porcine model of atherosclerosis. Phys Med Biol. 2009;54(18):5625-41.
10. Popele NM, Grobbee DE, Bots ML, Asmar R, Topouchian J, Reneman RS, et al. Association between arterial stiffness and atherosclerosis: the Rotterdam Study. Stroke. 2001;32(2):454-60.
11. Moore JE, Xu C, Glagov S, Zarins CK, Ku DN. Fluid wall shear stress measurements in a model of the human abdominal aorta: oscillatory behavior and relationship to atherosclerosis. Atherosclerosis. 1994;110(2):225-40.
12. Ando J, Yamamoto K. Effects of shear stress and stretch on endothelial function. Antioxid Redox Signal. 2011;15(5):1389-403.
13. Nerem RM, Levesque MJ, Cornhill JF. Vascular endothelial morphology as an indicator of the pattern of blood flow. J Biomech Eng. 1981;103(3):172-6.
14. Langille BL, Adamson SL. Relationship between blood flow direction and endothelial cell orientation at arterial branch sites in rabbits and mice. Circ Res. 1981;48(4):481-8.
15. Flaherty JT, Pierce JE, Ferrans VJ, Patel DJ, Tucker WK, Fry DL. Endothelial nuclear patterns in the canine arterial tree with particular reference to hemodynamic events. Circ Res. 1972;30(1):23-33.
16. Chien S. Mechanotransduction and endothelial cell homeostasis: the wisdom of the cell. Am J Physiol Heart Circ Physiol. 2007;292(3):1209-24.
17. Del CL, Sanchez LA, Salaices M, Kleeck RA, Exposito E, Gonzalez GC, et al. Vascular smooth muscle cell-specific progerin expression in a mouse model of Hutchinson-Gilford progeria syndrome promotes arterial stiffness: Therapeutic effect of dietary nitrite. Aging Cell. 2019;18(3):12936.
18. Wang JH, Goldschmidt CP, Wille J, Yin FC. Specificity of endothelial cell reorientation in response to cyclic mechanical stretching. J Biomech. 2001;34(12):1563-72.
19. Naruse K, Yamada T, Sokabe M. Involvement of SA channels in orienting response of cultured endothelial cells to cyclic stretch. Am J Physiol. 1998;274(5):1532-8.
20. Liu WF, Nelson CM, Tan JL, Chen CS. Cadherins, RhoA, and Rac1 are differentially required for stretch-mediated proliferation in endothelial versus smooth muscle cells. Circ Res. 2007;101(5):44-52.
21. Kamei M, Saunders WB, Bayless KJ, Dye L, Davis GE, Weinstein BM. Endothelial tubes assemble from intracellular vacuoles in vivo. Nature. 2006;442(7101):453-6.
22. Dvorak AM, Feng D. The vesiculo-vacuolar organelle (VVO). A new endothelial cell permeability organelle. J Histochem Cytochem. 2001;49(4):419-32.
23. Malek AM, Izumo S. Mechanism of endothelial cell shape change and cytoskeletal remodeling in response to fluid shear stress. J Cell Sci. 1996;109(4):713-26.
24. Helmlinger G, Geiger RV, Schreck S, Nerem RM. Effects of pulsatile flow on cultured vascular

endothelial cell morphology. J Biomech Eng. 1991;113(2):123-31.
25. Walpola PL, Gotlieb AI, Langille BL. Monocyte adhesion and changes in endothelial cell number, morphology, and F-actin distribution elicited by low shear stress in vivo. Am J Pathol. 1993;142(5):1392-400.
26. Zhao S, Suciu A, Ziegler T, Moore JE, Burki E, Meister JJ, et al. Synergistic effects of fluid shear stress and cyclic circumferential stretch on vascular endothelial cell morphology and cytoskeleton. Arterioscler Thromb Vasc Biol. 1995;15(10):1781-6.
27. Varandas E, Pereira HS, Monteiro S, Neves E, Brito L, Ferreira RB, Viegas W, Delgado M. Bisphenol A disrupts transcription and decreases viability in aging vascular endothelial cells. Int J Mol Sci. 2014;15(9):15791-805.
28. Collins C, Tzima E. Hemodynamic forces in endothelial dysfunction and vascular aging. Exp Gerontol. 2011;46(2-3):185-8.
29. Rennier K, Ji JY. Effect of shear stress and substrate on endothelial DAPK expression, caspase activity, and apoptosis. BMC Res Notes. 2013;6:10.
30. Bass GT, Ryall KA, Katikapalli A, Taylor BE, Dang ST, Acton ST, Saucerman JJ. Automated image analysis identifies signaling pathways regulating distinct signatures of cardiac myocyte hypertrophy. J Mol Cell Cardiol. 2012;52(5):923-30.
31. Jia G, Aroor AR, Jia C, Sowers JR. Endothelial cell senescence in aging-related vascular dysfunction. Biochim Biophys Acta Mol Basis Dis. 2019;1865(7):1802-9.
32. Tzur YB, Wilson KL, Gruenbaum Y. SUN-domain proteins: 'Velcro' that links the nucleoskeleton to the cytoskeleton. Nat Rev Mol Cell Biol. 2006;7(10):782-8.
33. Carey SP, Kraning RCM, Williams RM, Reinhart KCA. Biophysical control of invasive tumor cell behavior by extracellular matrix microarchitecture. Biomaterials. 2012;33(16):4157-65.
34. Jiang Y, Ji JY. Expression of Nuclear Lamin Proteins in Endothelial Cells is Sensitive to Cell Passage and Fluid Shear Stress. Cell Mol Bioeng. 2017;11(1):53-64.
35. Ives CL, Eskin SG, McIntire LV. Mechanical effects on endothelial cell morphology: in vitro assessment. In Vitro Cell Dev Biol. 1986;22(9):500-7.
36. Alessio P. Aging and the endothelium. Exp Gerontol. 2004;39(2):165-71.
37. Heyde C. Central limit theorem Encyclo Actuarial Sci. 2006.
38. Khatau SB, Hale CM, Stewart HPJ, Patel MS, Stewart CL, Searson PC, et al. A perinuclear actin cap regulates nuclear shape. Proc Natl Acad Sci U S A. 2009;106(45):19017-22.
39. Dahl KN, Booth GEA, Ladoux B. In the middle of it all: mutual mechanical regulation between the nucleus and the cytoskeleton. J Biomech. 2010;43(1):2-8.
40. Davidson PM, Lammerding J. Broken nuclei--lamins, nuclear mechanics, and disease. Trends Cell Biol. 2014;24(4):247-56.
41. Gregory TR. Coincidence, coevolution, or causation? DNA content, cell size, and the C-value enigma. Biol Rev Camb Philos Soc. 2001;76(1):65-101.
42. Ingber DE, Madri JA, Folkman J. Endothelial growth factors and extracellular matrix regulate DNA synthesis through modulation of cell and nuclear expansion. In Vitro Cell Dev Biol. 1987;23(5):387-94.

Cite this article as: Jiang Y, Witt N, Ji JY. Passage dependent changes in nuclear and cytoskeleton structures of endothelial cells under laminar shear stress or cyclic stretch. Int J Sci Rep 2021;7(6):327-39.